nature reviews chemistry

https://doi.org/10.1038/s41570-025-00779-3

Review article

Check for updates

The role of ionizing radiation-initiated reactions in targeted activation of chemotherapeutics

Juncheng Liu [1,2], Antonia G. Denkova [2] ✉ & Rienk Eelkema [1] ✉

Abstract

Ionizing radiation-induced drug release is a combined chemoradiation therapy, which aims to reduce the systemic toxicity of chemotherapeutics. Radiation is used for both radiotherapy and to trigger the release of a chemotherapeutic. To understand radiation-induced drug activation and to design new radiation-sensitive chemotherapeutics, it is important to become familiar with the underlying reaction mechanisms. Here, we provide an overview of the crucial process of water radiolysis induced by ionizing radiation and the mechanisms of reactive species generation. We also discuss the reactivity of these species with cellular components and chemical functional groups, to give insight into selective drug activation in complex cellular environments. Finally, we discuss recent progress on radiation-induced drug release focusing on the reaction of water radiolysis products with drug caging groups and the yield of released drugs. We aim to bridge the gap between basic chemical processes in water radiolysis and their relevance for drug release and provide suggestions on the design of radiation-sensitive prodrugs or nanocarriers.

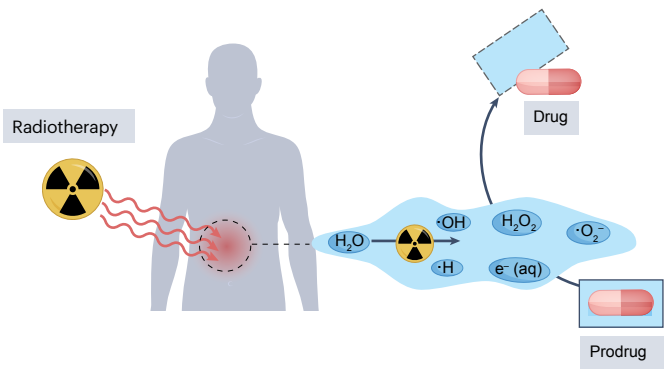

Sections

[1]Department of Chemical Engineering, Delft University of Technology, Delft, The Netherlands. [2]Department of Radiation Science and Technology, Delft University of Technology, Delft, The Netherlands. ✉e-mail: A.G.Denkova@tudelft.nl; R.Eelkema@tudelft.nl

Introduction

Surgery, chemotherapy and radiotherapy are the primary treatments for malignant tumours. Chemotherapy and radiotherapy have different cell-killing mechanisms and are, therefore, often used in combination to enhance therapeutic efficacy and minimize side effects[1]. Radiotherapy kills cancer cells either by direct interaction between radiation and DNA or indirectly by creating reactive species that then damage DNA. Radiation can be given externally, that is, in external-beam radiotherapy which uses high-energy photons, such as X-rays or γ-rays, or internally in radionuclide therapy that typically uses β^- particles, which have low linear energy transfer (LET). Such low-LET treatments result mostly in indirect damage to DNA via radical formation. Alternatively, high-LET radiation (for example, α-particles) induces mostly direct DNA damage, which is often clustered and therefore difficult to repair.

Chemotherapy uses cytotoxic drugs to treat localized tumours or metastasized cancer, inducing cell death or inhibiting proliferation[2]. However, the systemic administration of chemotherapeutics means also treating normal tissues and results in severe side effects. These side effects affect patient well-being and limit both the dose of administered drug and treatment duration[3]. Enhancing the effectiveness of cancer therapy requires either increasing the effects on tumours or reducing the impact on surrounding tissues[4]. Stimuli-induced drug release from nanocarriers and prodrugs offers a way to reduce the side effects to healthy tissues by releasing active drugs only in response to conditions specific to tumours such as low pH[5], hypoxia[6] and enzymes[7]. External release stimuli such as near-infrared light[8] and ultrasound[9] have also been extensively studied in the treatment of various types of cancers[10].

The combination of radiotherapy and systemic drug administration has various treatment consequences[11,12]. For example, treating a tumour with radiation perturbs the cell cycle[13], making the tumour more sensitive to chemotherapeutics. Drug release triggered by ionizing radiation offers important advantages over traditional combinations of radiotherapy and chemotherapy. It can exploit the different therapeutic mechanisms of the two treatments, potentially reducing the systemic toxicity of antitumour drugs and enhancing overall treatment efficacy. Various drug carriers have been reported for ionizing radiation-initiated drug release system, including metal-organic frameworks[14,15], covalent organic frameworks[16], polymeric nano-aggregates[17–19] and prodrugs[20,21]. Besides, radiation-induced versions of photodynamic therapy[22–26] and radiation-activated scintillating nanoparticles[27,28] have also been reported. In contrast to radiation-initiated photodynamic therapy effects — in which heavy elements with high cross-sections are used to convert the energy from radiation to photosensitizers[29] — activation of prodrugs relies on chemical reactions with species generated by the radiolysis of water, as most prodrugs (organic compounds) do not absorb radiation to any appreciable degree.

The interaction of these therapies with various cell lines or tumours has been discussed in recent reviews[30–34]. However, these reviews primarily focused on novel chemistries and drug release applications, while giving limited attention to the fundamental mechanisms of water radiolysis and the interactions of reactive species with functional groups — processes that are crucial for advancing scientific understanding and progress in this field. In this Review, we aim to bridge this gap, to help researchers to rationally develop new radiation-induced drug release systems. We will start with the fundamentals of radiation chemistry, discussing the physical processes and chemical reactions taking place on the sub-picosecond to pseudo-steady-state microsecond timescales. On the microsecond timescale, scavengers and prodrugs are able to react with species from water radiolysis (for example, aqueous electron, hydroxyl radical and hydrogen peroxide). We will discuss the radiolytic yields and reactivity of these species and discuss which species, as a result, is more relevant for triggering drug release. As the drug release has to be performed in the tumour microenvironment, the compatibility and limitations of these species will be discussed to give an expectation of the yield of the released drug. Finally, we will discuss boundary conditions of radiation-initiated drug release systems, illustrated by recently published examples. Through this Review, we aim at providing deeper understanding in radiation-induced drug release from the perspective of radiation chemistry and eventually to the rational design of new drug delivery systems.

The basics of radiation chemistry

Before discussing the radiation-initiated chemical processes of drug release from prodrugs and nanocarriers, it is essential to briefly introduce the fundamentals of radiation chemistry in aqueous solutions. A key characteristic of ionizing radiation is that the initial interaction of radiation with matter depends on the atomic makeup of the matter and much less on the molecular structure[35]. Therefore, radiation energy is absorbed by the molecules present in the system in proportion to their atomic weight and relative abundance, and energy absorption is most likely to result in the ejection of an electron. In the case of irradiation of dilute aqueous solutions ([solute] < 0.1 M), generally speaking, only water molecules ([water] = 55 M in aqueous solutions) are ionized, and any subsequent radiation-initiated reactions are mediated by the products of water radiolysis[36,37]. Therefore, understanding the radiation chemistry of water radiolysis is crucial in the design of radiation-activated prodrugs[38,39].

Interactions of ionizing radiation with water

Figure 1 outlines the physical and chemical processes that occur following the irradiation of water[37]. The primary processes are the interactions of high-energy photons (such as γ-rays and X-rays) or charged particles (such as electrons, protons and α-particles) with water, resulting in electronic excitation (reaction **1**) or ionization (reaction **2**). The H_2O^+ produced in reaction **2** undergoes an ion-to-molecule reaction with another water molecule to form ·OH and H_3O^+ (reaction **3**). The ejected electron from reaction **2** may cause a secondary ionization and, in the end, can be trapped by surrounding water to form a so-called aqueous electron (e^-_{aq}, reaction **5**). The H_2O^* (excited water) disassociates to ·OH and ·H (reaction **4**). Reactions **1**–**5** take place on a timescale of 10^{-16}–10^{-12} s, after which the radicals start to diffuse randomly. At the start of the diffusion process (10^{-12} s), the radicals may encounter one another and undergo reaction **6**–**12** (10^{-12}–10^{-7} s). Next, the species diffuse homogeneously in the solution and react with solutes (for example, prodrugs or scavengers) within 10^{-4} s. After that, all the radicals are quenched or recombined to form molecular products.

Among all the products formed by water radiolysis, the species most likely to initiate chemical reactions (for example, activating prodrugs) are e^-_{aq}, ·OH, ·H and H_2O_2. The radiolytic yield of H^+ is too small to induce a significant pH change in biological systems and is thereby not suitable for such applications. The reaction rate between prodrugs and radiolytic species is generally below 10^7 s^{-1} (see the section Reactivity and selectivity of radiolytic species in biological systems)[36], meaning that anything lasting less than 10^{-7} s does not react sufficiently fast enough to contribute significantly to the

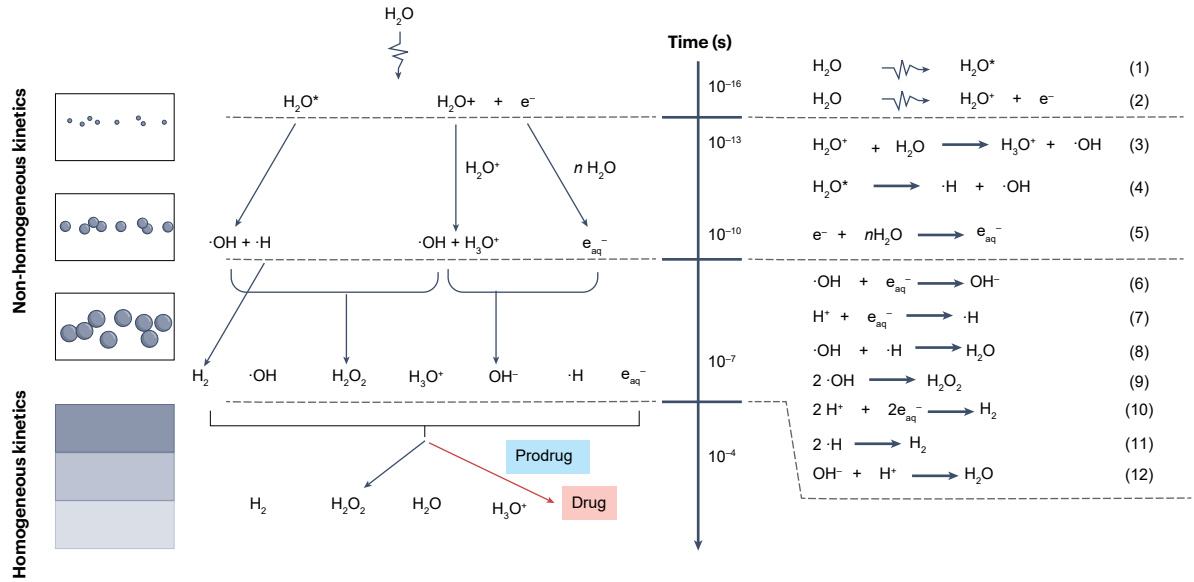

Fig. 1 | Time-dependent events of water radiolysis and the related reactions. The grey area indicates the spatial distribution of radicals: at timescales from 10^{-16} to 10^{-7} s, the radical distribution looks like spurs in which reactions have non-homogeneous kinetics; at timescale > 10^{-7} s, radicals distribute homogeneously in solution[37].

product distribution. This means that the yield of reactive species that persist longer than 10^{-7} s determines the expected yield of activated drugs.

Radiolytic yield of reactive species

The interaction of ionizing radiation with water results in multiple water molecules being ionized or excited by a single ionizing event. LET describes the energy absorbed by matter (in this case, water) as a function of travelled distance of incident radiation, which determines the number of ionizations along the track[40]. For low-LET radiation (photons and high-energy electrons), ionizations are widely spread along the track, and the diffusion pattern of radicals resembles a spur (tiny regions with high concentrations of radicals, Fig. 1). As spurs are far away from each other, radical recombination between spurs is limited, so radical products (for example, e^-_{aq}, ·H and ·OH) are favoured over molecular products. Conversely, high-LET radiation tends to produce more of the molecular products (for example, H_2 and H_2O_2) and less of the radical products[41,42], as spurs occur close to each other thus facilitating radical recombination.

The dose of radiation is given by the unit Gray (Gy), in which 1 Gy equals 1 J of energy absorbed by 1 kg of matter (1 Gy = 1 J kg^{-1}). The radiolytic yields, known as *G*-values, are expressed as the number of molecules formed per 100 eV of absorbed energy, in which 1 molecule per 100 eV is approximately equal to 0.103 μmol J^{-1}, and 0.103 μM Gy^{-1} for solutions of unit density (for example, water when ρ = 1 kg L^{-1})[43]. In aqueous solutions with low concentration of scavengers (less than tens of millimolar concentration), the *G*-values of reactive species that remain after 10^{-7} s timescale are close to the values shown in Table 1. Clinical administration of concurrent chemoradiation therapy follows a fractionation regimen, that is, radiation is given in several fractions[44,45]. Long-course chemoradiotherapy generally delivers 40–60 Gy in approximately 30 fractions over 5–6 weeks, whereas short-course combination therapy delivers ~25 Gy in 4–5 fractions over 3 weeks[46]. For each fraction, the delivered dose varies from 2 Gy to 10 Gy, where ~0.56–2.8 μM of e^-_{aq}/·OH is generated.

The reactivity of products of water radiolysis

In this section, we will discuss the products of water radiolysis, relevant for triggering prodrug activation. These species include radical products such as e^-_{aq}, ·OH and H·, as well as the molecular product H_2O_2. Given the reactivity of these species with a broad range of substrates, we will discuss the reaction rates of each species with various typical substrates or functional groups. The second-order reaction rate constants are listed in Supplementary Tables 1 and 2 and summarized in Fig. 2. The data are acquired from ref. 47. Here, we will focus on the reactions of the most relevant water radiolysis products with:

1. compounds abundant in cellular components, such as amino acids, lipids, carbohydrates and nucleotides;
2. typical reactive functional groups, for example, nitro compounds with aqueous electrons;
3. functional groups that have been used recently to design radiation-sensitive prodrugs.

By comparing these reaction rates, we expect that readers will be able to estimate which reaction will dominate in a given system such as the tumour microenvironment. Moreover, understanding the reaction mechanisms of these reactive species can help anticipating the final product, providing in this way considerations for prodrug design.

Table 1 | *G*-values for water radiolysis for low-linear energy transfer radiation

Reactive species	e^-_{aq}	·OH	·H	H_2O_2
Yield (μM Gy^{-1})	0.28	0.28	0.062	0.073
Yield (molecule per 100 eV)	2.70	2.70	0.060	0.70

Aqueous electron

The aqueous electron is a strong reductant with a reduction potential of −2.9 V (versus H^+/H_2), which readily reduces metal ions (equation (13), Fig. 2c). For example, e^-_{aq} can reduce Cu(II) to Cu(I) at a diffusion-controlled rate ($k = 3.3 \times 10^{10}\ M^{-1}\ s^{-1}$; Fig. 2a and Supplementary Table 1). Aqueous electrons are unreactive towards saturated hydrocarbons,

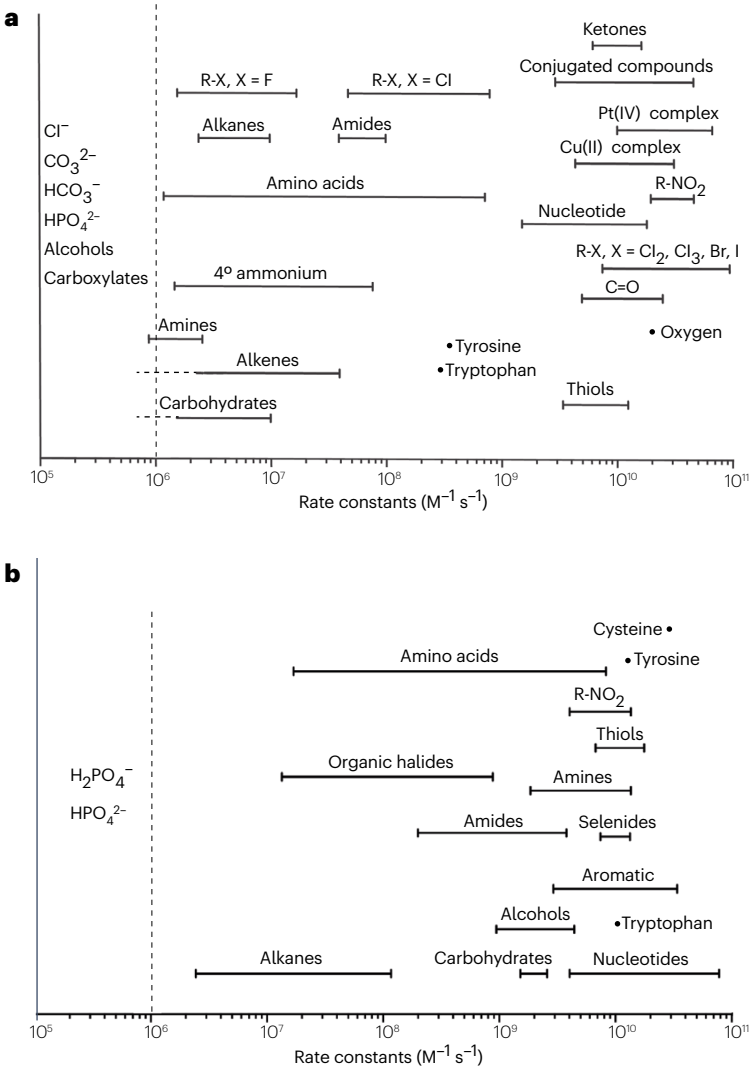

Fig. 2 | Reactivity of species generated through water radiolysis. **a**, Second-order rate constants for reactions of aqueous electrons in aqueous solutions[47,111], summarized from Supplementary Table 1. Species on the left of the dashed line can be considered unreactive. **b**, Second-order rate constants for reactions of hydroxyl radical in aqueous solution[47], summarized from Supplementary Table 2. **c**, Equations (13) to (17) show typical reactions with aqueous electrons and hydroxyl radicals.

c

$$M^{n+} + e^-_{aq} \longrightarrow M^{(n-1)+} \quad (13)$$

$$CR{-}X + e^-_{aq} \longrightarrow {\cdot}CH_2R + X^- \quad X = F, Cl, Br, I \quad (14)$$

$$RR'C{=}O + e^-_{aq} \longrightarrow RR'\dot{C}{-}O^- \quad (15)$$

$$RHC{=}CHR' + {\cdot}OH \longrightarrow RH\dot{C}{-}\overset{OH}{\overset{|}{C}}HR' \quad (16)$$

$$RR'HC{-}H + {\cdot}OH \longrightarrow RR'HC{\cdot} + H_2O \quad (17)$$

isolated alkenes, alcohols, amide bonds and amines, meaning that cellular components such as lipids, sugars, most of the amino acids (with exception of cystine and cysteine) and peptides are inert to e^-_{aq} (Fig. 2a). In aqueous solutions, e^-_{aq} interacts with organic compounds primarily through two mechanisms[48,49]: (1) dissociative electron capture (equation (14), Fig. 2c) and (2) addition reactions to π-bonds (equation (15), Fig. 2c). A common reaction involving e^-_{aq} is the electron capture by a carbon–halogen bond, resulting in the release of a halogen anion and production of a carbon-centred radical. The reaction rate can vary by four orders of magnitude depending on the structure. Fluorinated compounds are less reactive than other organic halides. Bromo and iodo-compounds react rapidly with e^-_{aq}, whereas the degree of substitution determines the reaction rate of organochlorides (Supplementary Table 1). Compounds containing electron-withdrawing groups demonstrate high reactivity towards e^-_{aq}. For examle, both aliphatic and aromatic nitro compounds react with e^-_{aq} in diffusion-controlled reaction rates (~10^{10} M^{-1} s^{-1}). π-Conjugated compounds with electron-withdrawing groups are also reactive to e^-_{aq}, with k ~ 10^9–10^{10} M^{-1} s^{-1}. In biological systems, e^-_{aq} reacts rapidly with electron-deficient nucleobases (k ~ 10^{10} M^{-1} s^{-1}). Additionally, the aqueous electron can perform one-electron reduction of thiols (for example, cysteine, $k = 1.2 \times 10^{10}$ M^{-1} s^{-1}) or disulfides (for example, oxidized glutathione, $k = 3.7 \times 10^9$ M^{-1} s^{-1}) through dissociative electron transfer mechanisms, leading to the formation of thiol radicals (Fig. 2a). It is important to note that e^-_{aq} reacts with molecular oxygen at a diffusion-controlled rate, to form a peroxyl anion known as superoxide. Superoxide is a highly reactive species, which is quickly scavenged by superoxide dismutase in living organisms. The concentration of molecular oxygen can vary substantially depending on the type of tissue: the average physiological oxygen level in normal tissues is ~5% (~60 μM) ('normoxia'), whereas in cancerous tissues it typically drops to <2% (~25 μM) ('hypoxia'). Certain tumour types or zones can be extremely hypoxic, with oxygen levels falling below 0.5% (Fig. 2a).

Hydroxyl radical

OH reacts with most organic substrates at close to diffusion-controlled rates, which includes, for example, alcohols, carbohydrates, thiols, aromatic compounds and organic selenides (Fig. 2b). Among these, electron-rich aromatic compounds (such as methoxyphenols and methoxybenzoates) and organic selenides have even higher reaction rates (k-10^{10} M^{-1} s^{-1}) with ·OH. By contrast, ·OH is relatively inert to organic halides (~10^8 M^{-1} s^{-1}). The main reaction types of ·OH with substrates include (1) addition to double bonds, (2) hydrogen abstraction and (3) electron transfer[50] (Fig. 2c). In biological systems, ·OH undergoes addition reactions with double bonds in the base moieties of nucleotides[51] (equation (16), Fig. 2b) with near diffusion-controlled rate constants (k ~ 10^{10} M^{-1} s^{-1}). Additionally, ·OH participates in hydrogen abstraction reactions at the sugar moiety (equation (17), Fig. 2b,c), such as glucose ($k = 1.5 \times 10^{10}$ M^{-1} s^{-1}) and ribose ($k = 1.5 \times 10^{10}$ M^{-1} s^{-1}). Given the relatively high concentration of nucleotides in cells and the rapid reaction rate of ·OH with most biological molecules, the design of prodrugs or activation systems targeted by ·OH should incorporate functional groups that are either present in significantly higher concentrations than nucleotides or have a much higher reaction rate with ·OH. The section 'Radiation-initiated drug release' will present a few examples using ·OH as the triggering agent:

Hydrogen radical

The hydrogen radical (H·) is the conjugate acid of e^-_{aq}, with a pK_a of 9.1. The typical reaction of H· with organic compounds is hydrogen abstraction, which occurs at a significantly lower rate compared with reactions with ·OH (ref. 47). Under physiological conditions, e^-_{aq} is considered the dominant reductant, which is attributed not only to the lower radiolytic yield of H· compared with e^-_{aq} but also to the fact that the reaction rates of H· with most organic compounds are one to three orders of magnitude lower than those of e^-_{aq}.

Hydrogen peroxide

Hydrogen peroxide is present in most cells at concentrations ranging from a few micromolar in normal cells to sub-millimolar in cancerous or inflamed cells[52,53]. This widespread presence makes H_2O_2 a popular stimulus for activating prodrugs or nanocarriers[54,55]. However, the radiolytic production of H_2O_2 under low-LET radiation has a very low yield (0.07 μM Gy^{-1}), leading to radiation-induced concentrations that are comparable to typical intracellular levels. Consequently, designing prodrugs that rely on H_2O_2 generated by low-LET radiation is quite challenging. There are, to the best of our knowledge, no examples published that use H_2O_2 generated from water radiolysis. By contrast, high-LET radiation produces somewhat higher yields of H_2O_2 (for example, 0.13 μM Gy^{-1} for 3.4 MeV α-beams)[56,57], making it useful to consider in combination with radionuclide therapy.

Reactivity and selectivity of radiolytic species in biological systems

As discussed in the previous section, both e^-_{aq} and ·OH can react with a wide variety of cellular components. In this section, we will discuss the selectivity of their reactions with cellular components and radiolytic species-sensitive molecules. Consider a prodrug is designed to react with e^-_{aq}, exposure of a biological system containing this prodrug to ionizing radiation generates e^-_{aq}, which can then react with either the prodrug molecule or any other cellular components. The fraction (f) of e^-_{aq} reacting with the prodrug relative to the overall scavenging by cellular components can be used to quantify the reactivity of the prodrug in a biological system[58].

f is given by:

$$f = k_p[\text{functional group}]/\sum(k_i[S_i]) \tag{18}$$

and the generated concentration of the activated drug is given by:

$$[\text{activated functional group}] = [e^-_{aq}] \times f \tag{19}$$

in which k_p is the rate constant of e^-_{aq} with functional group, k_i is the reaction rate of the ith cellular component S_i with e^-_{aq}, $[e^-_{aq}]$ is the yield of aqueous electrons at a given dose of radiation. The sum represents all the scavenging reactions of e^-_{aq} within cells, including the reaction with the prodrug. In 1978, Michaels and Hunt[59] estimated this sum to be 3.4×10^8 s^{-1} in mammalian cells without prodrugs. This estimation is based on several assumptions, including the homogeneous distribution of all reactants within cells. However, certain scavengers, such as bases in DNA, are concentrated in the nucleus and are not homogeneously distributed, suggesting that the actual value might be lower. Considering a few homogeneously distributed e^-_{aq} scavengers in cancerous tissues, such as glutathione (intracellularly 1–10 mM (ref. 60) and 20–40 μM outside cells[61,62], $k = 4.5 \times 10^9$ $M^{-1}s^{-1}$), cysteine (~0.3 mM in blood[63,64], $k = 1.2 \times 10^{10}$ M^{-1} s^{-1}) and oxygen (on average 16.3 μM (ref. 65) in tumour microenvironment, $k = 1.9 \times 10^{10}$ M^{-1} s^{-1}) and using the previously mentioned reaction rates, the sum is 0.40×10^7 s^{-1} (outside cells). In this context, substantial activation of a prodrug by e^-_{aq} requires that

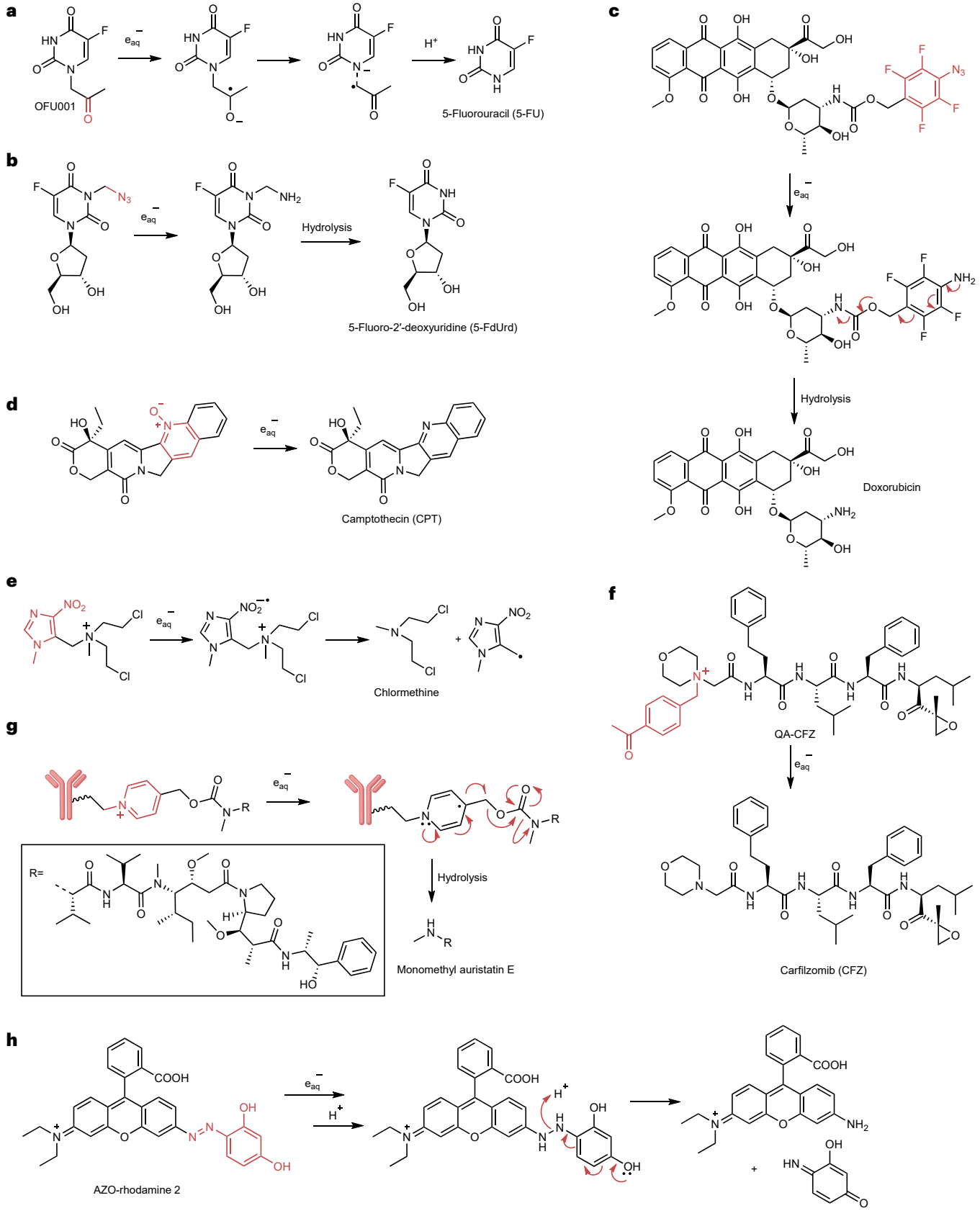
a
OFU001
5-Fluorouracil (5-FU)
b
Hydrolysis
5-Fluoro-2′-deoxyuridine (5-FdUrd)
c
Hydrolysis
Doxorubicin
d
Camptothecin (CPT)
e
Chlormethine
f
QA-CFZ
Carfilzomib (CFZ)
g
R=
Hydrolysis
Monomethyl auristatin E
h
AZO-rhodamine 2

Fig. 3 | Prodrug activation induced by aqueous electrons. a, Activation of 2-oxoalkyl-caged 5-FU via cleavage of C–N bond induced by aqueous electrons. **b**, Reduction of azido methyl group by aqueous electrons followed by hydrolysis and releasing 5-FdUrd. **c**, Reduction of 2,3,5,6-tetrafluorophenyl azide followed by the hydrolysis of a self-immolative carbamate linker to release Dox. **d**, Reduction of *N*-oxide to release camptothecin. **e**, Reduction of 2-nitropyrrole-induced C–N bond cleavage and the release of chlormethine. **f**, Aqueous electrons induced decaging of *p*-acetylbenzyl ammonium to release carfilzomib. **g**, Cleavage of the C–N bond of a picolinium group and the rearrangement of the resulting compound to release monomethyl auristatin E. **h**, Reduction and immolation of an aryldiazo group to form an amine functionality. CFZ, carfilzomib.

k_p[functional group] should be at least comparable to this value. In the case of a prodrug designed to react with ·OH, the competition between the prodrug and cellular components for ·OH is less favourable, as sugars, which are unreactive to e^-_{aq}, can rapidly react with ·OH. Considering some homogeneously distributed ·OH scavengers in cells, such as cysteine ($k = 3.4 \times 10^{10}\ M^{-1}\ s^{-1}$), glucose (~5.5 mM (ref. 66), $k = 1.5 \times 10^{9}\ M^{-1}\ s^{-1}$) and glutathione ($k = 1.4 \times 10^{10}\ M^{-1}\ s^{-1}$), the total scavenging rate is $1.91 \times 10^{7}\ s^{-1}$. This rate is more than four times higher than that of e^-_{aq}, making the design of prodrugs targeted by ·OH significantly more challenging than those targeting e^-_{aq}.

Guidelines for the design of radiolysis-driven drug activation systems

Given their substantially higher radiolytic yield, e^-_{aq} and ·OH are preferred over other radiolysis products as species initiating release, and prodrugs should be designed to react rapidly and selectively with these species. To achieve any required amount of drug activation (equations (18) and (19)), the prodrug must have a significantly higher reactivity than the combination of scavengers present. As the concentration of prodrugs (~10^1 μM) is much lower than that of scavengers (<10 mM), the reaction rate of the prodrug should be at least one order of magnitude higher than that of the scavengers. Any combination of functional group concentration and rate constant (Figs. 2 and 3) that satisfies this condition has the potential to act as a radiolysis product-sensitive functional group. Reaction of such a functional group with the radiolysis product should lead to bond breakage (for example, diselenide or stilbene), group transformation (for example, *N*-oxide to amine) or initiation of a self-immolation process (for example, azidobenzyl to aminobenzyl and subsequent removal of the cage). The prodrug should have good solubility to ensure a homogeneous reaction with reactive species. The drug should be effective at the concentrations predicted by equations (18) and (19), and the prodrug should have only limited toxicity at the applied concentration.

Challenges for clinical translation

The ultimate goal of these developments is clinical translation, that is, the application of radiation-triggered drug release strategies in patients to treat cancer through the combination of radiotherapy with chemotherapy or immunotherapy. To date, this approach has not yet entered clinical trials, which is understandable given that the field remains in its early stages of development. Nevertheless, several key challenges must be addressed to enable successful clinical implementation.

First, drug release must be achieved at clinically relevant radiation doses, typically ranging from 2 Gy to 10 Gy for external beam therapy and up to several tens of Gray for radionuclide therapy[67,68]. Second, the prodrug must exhibit minimal inherent toxicity, whereas the released drug must demonstrate high therapeutic efficacy — in other words, the prodrug–drug system should offer a large therapeutic index. In addition, the prodrug must remain stable under physiological conditions in the absence of radiation, avoiding premature hydrolysis or degradation. By-products generated by the activation must also be non-toxic and should not induce undesirable side effects. The timing of drug release is another critical factor: tumour uptake and retention of the prodrug must be sufficient and well characterized to enable effective combination with radiotherapy. Although addressing these challenges is complex, the flexibility provided by the range of available radiation-cleavable groups and therapeutic agents offers opportunities to facilitate eventual clinical translation. Furthermore, the dose-limited generation of radiolytic species and the presence of intracellular scavengers put a limit on the achievable concentration of activated drugs and may necessitate the use of highly potent drugs (for example, monomethyl auristatin E, MMAE) or self-immolative strategies that enable the release of multiple therapeutic molecules following a single triggering event. The potential toxicity of by-products can often be predicted based on their known reactivity with organic molecules, facilitating the rational design of inherently safe prodrugs. When designing these prodrugs, it is essential to optimize biodistribution, favouring routes such as renal clearance, and to achieve pharmacokinetics that allow for sufficient tumour uptake and retention. Although some predictions regarding biodistribution can be made based on the molecular structure of the prodrug candidates, experimental validation in animal models will be necessary to identify the most effective designs.

Radiation-initiated drug release

In the previous section, we discussed the selectivity of e^-_{aq} and ·OH towards radiation-sensitive molecules in biological systems. We will now discuss examples in which different functional groups have been designed to react with e^-_{aq} and ·OH (Table 2). After exposure to ionizing radiation, the reactions of radiolytic species with these functional groups induce molecular changes in the parent molecule, leading to drug release. By critically reviewing published papers from a radiation chemistry perspective, we aim to provide insights and inspiration for the design of effective radiation-initiated drug release systems.

Carbonyl compounds

Shibamoto et al.[69] were among the first to report a radiation-activatable prodrug OFU001 (Fig. 3a), which was constructed by protecting the antitumour drug 5-fluorouracil (5-FU) at the N(1) position using a 2-oxoalkyl group. Under X-ray irradiation, the formed e^-_{aq} added to the carbonyl group to form a π* anion radical, which is further thermalized to the σ* orbital with a weak C–N bond, followed by the dissociation of the C–N bond and the release of 5-FU. Release of 5-FU was substantially enhanced under irradiation in hypoxic conditions, with a *G*-value of 0.19 μM Gy^{-1}, whereas the *G*-value was 0.010 μM Gy^{-1} in aerobic conditions, underlining the scavenging propensity of molecular oxygen. With the decent radiolytic yield of 5-FU, the authors tested the cytotoxicity of the prodrug under irradiation with X-rays. OFU001 showed much lower toxicity compared with 5-FU, and the cell surviving fraction dropped significantly in the group of OFU001 with 30 Gy of irradiation under hypoxic conditions. However, it should be noted that these

Table 2 | Summary of key parameters of each strategy

Caging group	Reactive species	Source of radiation	Dose (Gy)	*G*-value of drug	Cell line	Animal model	Ref.
Carbonyl compounds	e^-_{aq}	X-ray	7.5–30	0.19 μmol J^{-1} (hypoxic) 0.01 μmol J^{-1} (aerobic)	SCCVII	Not available (NA)	110
Azido compounds	e^-_{aq}	X-ray	6	0.159 μmol J^{-1} (hypoxic) 0.05 μmol J^{-1} (aerobic)	A549	NA	72
2,3,5,6-Tetrafluorophenyl azide	e^-_{aq}	X-ray	6	Not detected (ND)	HeLa	BALB/c nude mice	73
2,3,5,6-Tetrafluorophenyl azide	e^-_{aq}	X-ray	10	ND	MCF-7	BALB/c nude mice	74
Azido compounds	e^-_{aq}	X-ray	3–4	ND	CT26	BALB/c mice	75
N-oxide	e^-_{aq}	X-ray	4 Gy for 4 fractions	0.14 μM Gy^{-1}	CT 26; HCT 116	BALB/c nude mice	77
N-oxide	e^-_{aq}	X-ray	10	0.12 μM Gy^{-1}	BM-DC	C57BL/6J mice	78
N-alkoxy	e^-_{aq}	X-ray	1	>24.6 μM Gy^{-1}	NA	NA	80
Nitroaryl methylquaternary ammonium	e^-_{aq}	γ-rays from Co-60	Not mentioned	0.67 μmol J^{-1}	NA	NA	81
p-Acetylbenzyl-substituted ammonium	e^-_{aq}	X-ray	4 Gy for 4 fractions	0.16 μM Gy^{-1}	CT 26; HCT 116; HeLa	BALB/c mice	82
Picolinium	e^-_{aq}	X-ray	4 Gy for 3 fractions	0.137 μM Gy^{-1}	U87MG; HT1080-FAP; 4T1-FAP	BALB/c mice	83
Azo compound	e^-_{aq}	X-ray	4–40 Gy	0.14 μM Gy^{-1}	NA	NA	84
Cobalt(III) complex	e^-_{aq}	γ-rays from Co-60	15 Gy	0.17 μmol J^{-1}	AA8; UV4; SKOV-3; EMT6-V	NA	85
$Pd(II)(OAc)_2$	e^-_{aq}	γ-rays from Co-60	1–20 Gy	2.75 μM Gy^{-1}	A549	NA	87
$OxaliPt(IV)\text{-}(OAc)_2$	e^-_{aq}	X-ray	4 Gy for 4 fractions	ND	HCT116; LoVo; Ls513; HT29; BGC823; MC38		88
Dihydroxylbenzyl compounds	·OH	γ-rays from Co-60 and X-ray	4 Gy	0.04 μM Gy^{-1}	4T1; HeLa; MC38	NA	89
Benzothiazoline compounds	·OH	γ-rays	0–110 Gy	ND	NA	NA	90
Organochloride	e^-_{aq}	γ-rays from Co-60 and X-ray	0–60 Gy	ND	NA	NA	104
Organo diselenide	·OH	γ-rays from Co-60	5 Gy	ND	HepG2	NA	97
Organo tellurium	·OH	γ-rays from Co-60	2 Gy	ND	NA	NA	100
Disulfide	e^-_{aq}/H	X-ray	6–9 Gy	ND	A549	NA	103

experiments were performed by first irradiating prodrug in Eagle's minimum essential medium which was then added to the cells, which is not clinically applicable. Although there has been follow-up research using the carbonyl group as a drug-caging group[70], the activation efficiency in biological systems is far below than what is needed. This negative result may be caused by competition reactions of various cellular components in tissues, reducing the utility of the carbonyl group as a prodrug cage. In other words, the decaging reactions of prodrugs should out-compete the scavenging reactions in biological systems to make the drug release efficient.

Azido compounds

Azides (RN_3) are known to be reduced to amines (RNH_2) by reductants such as H_2S, H_2 and phosphines[71]. Tanabe et al.[72] showed that the reduction can also be triggered by reducing species from the radiolysis of hypoxic water such as e^-_{aq}. They designed a prodrug in which 5-fluoro-2′-deoxyuridine (5-FuUrd) was protected by an azido methyl group (Fig. 3b). Upon reacting with e^-_{aq}, the azido group was reduced to the amino compound and the formed methylamino group underwent a hydrolysis reaction to release 5-FdUrd. The *G*-value of the reaction was 0.16 μM Gy^{-1}. A549 cells first treated with N3-FdUrd and irradiated for 6 Gy showed significant difference in cell viability ($P < 0.05$) compared with the N3-FdUrd negative group. The reactivity of azido group increases when it is connected with electron-withdrawing group. Geng et al.[73] demonstrated that sulfonyl azides and 2,3,5,6-tetrafluorophenyl azides can be reduced to amines under hypoxic irradiation. The *p*-azido-2,3,5,6-tetrafluorobenzyl caging group can be reduced to an aniline, which subsequently undergoes 1,6-self-immolation to release doxorubicin (Dox) (Fig. 3c). The radiolytic yield of the drug was ~5 μM after exposure to 60 Gy of X-irradiation (~0.083 μM Gy^{-1}).

Recent years have witnessed the wide application of radiation-reduced azido compounds for the combination of radiotherapy with not only chemotherapy but also immunotherapy and proteolysis targeting chimera (PROTAC) prodrugs. For example, Yang et al.[74] reported a radiation-inducible PROTAC molecule (RT-PRO), in which

the VHL E3 ligase-targeted hydroxyl group of the parent PRO was caged by a 2,3,5,6-tetrafluorophenyl azide moiety. The treatment of RT-PRO + X-ray showed significant growth inhibition both in vitro (MCF-7 cells) and in vivo (MCF-7 bearing BALB/c nude mice). Sun et al.[75] reported an azido-functionalized resiquimod (R848-N_3) that in its prodrug form has a greatly reduced inflammatory effect (cytokine storm). Following radiotherapy, the concentration of activated resiquimod in the tumour was 11-fold higher than that in the liver at 24 h. Elevated levels of immune cells were observed in both primary and secondary tumours, demonstrating a robust systemic antitumour effect.

N-oxides

N-oxide derivatives, such as tirapazamine, were initially used as effective hypoxia-targeting agents owing to their efficient reduction by cellular reductases[76]. The so-formed benzotriazinyl radical performs hydrogen abstraction from DNA, leading to strand breaks. Ding et al.[77] creatively applied *N*-oxide derivatives in radiation-activated prodrug therapy. They hypothesized that the e^-_{aq} generated from water radiolysis could reduce *N*-oxides to tertiary amines (Fig. 3d). They suggested that the e^-_{aq} first occupies the π orbital of the *N*-oxide by a tunnelling effect. Additionally, *N*-oxides with extended π systems increased the reactivity of e^-_{aq} to *N*-oxide. Through structural screening, they identified aniline *N*-oxides and aromatic heterocyclic *N*-oxides as promising groups for the reaction, with *G*-values close to the *G*-value of e^-_{aq} in phosphate-buffered saline (PBS). Antitumour drugs such as camptothecin (CPT), which contain heterocyclic tertiary amines, were used as drug candidates in this study. The IC_{50} of the prodrug NO-CPT was 22-fold lower than that of CPT against the CT26 cell line. Tumour-bearing mice treated with NO-CPT and fractionated radiotherapy (4 Gy per fraction) showed significantly greater tumour growth suppression. This concept was recently extended to the activation of TLR7/8-agonists for cancer immunotherapy[78,79]. Analogous to *N*-oxide reduction by e^-_{aq}, Anderson et al.[80] recently reported an X-ray-triggered release of quinoline-based drugs from *N*-alkoxyquinoline prodrugs, in which a radical chain reaction can lead to yields that greatly exceed the stoichiometric maximum *G*-value, albeit only under anaerobic conditions.

Nitroaryl compounds

Kriste et al.[81] reported prodrug activation exploiting the reduction of nitroaryl methylquaternary ammonium salt by e^-_{aq} (Fig. 3e). The formed nitro radical anion undergoes rearrangement to break the C–N bond of a quaternary ammonium salt, resulting in the release of a tertiary amine derivative. They used the chlormethine nitrogen mustard as the model drug. For the protecting group, they examined a series of nitrophenyls and nitroheterocycles and found the kinetics of fragmentation reactions varied by more than four orders of magnitude independent of reduction potential. 4-Nitroimidazole provided efficient chlormethine release with *G*-value of 0.67 μmol J^{-1} in deaerated water with 0.1 M sodium formate buffer and 5 mM sodium phosphate (pH = 7.0). The high *G*-value suggests that other pathways contribute to release. However, the toxicity of this series of prodrugs was only 1.3–5.6 times lower than the corresponding drug, limiting the application potential of this prodrug cage.

Quaternary ammonium compounds

Generally, quaternary ammonium salts such as tetrabutylammonium ion are unreactive to aqueous electrons (Fig. 2a). However, Guo et al.[82] reported that *p*-acetylbenzyl-substituted ammonium salts had a much higher reactivity towards aqueous electrons because of their high electron affinity, with reduction resulting in the cleavage of the *p*-acetylbenzylic bond. The cleavage reaction also worked on a carfilzomib (CFZ)-based prodrug QA-CFZ (Fig. 3f). In vitro experiments showed that the *G*-value of carfilzomib activation is ~0.16 μM Gy^{-1} in PBS. Tumour-bearing mice showed larger tumour-growing suppression in the group treating with QA-CFZ and 4 Gy of X-ray irradiation.

The same group reported another prodrug activation method using the reaction of e^-_{aq} with picolinium derivatives[83] (Fig. 3g). The positive charge of picolinium makes it more reactive than picolyl or quinolinyl substitution. The formed electrically neutral radical underwent rearrangement to release the parent drug. The *G*-value of released drug was 0.137 μM Gy^{-1} in phosphate buffer (pH 7.4), to *G*-value e^-_{aq}. An antibody–drug conjugate (ADC) consisting of a fibroblast activation protein-targeted antibody and MMAE was synthesized using such a functional group as the linker. The ADC reached maximum tumour accumulation on the second day; at this point, radiation was applied. The radiolytic yield of released MMAE was 0.035 μM Gy^{-1}. Tumour-bearing mice treated with ADC and radiation showed lower tumour volume but similar body weight compared with single treatment groups. This example demonstrated that although the radiolytic yield of drugs in tissue was lower than that in phosphate buffer because of the scavenging reactions we discussed previously, the tumour-killing efficiency was still significantly higher than when only using radiotherapy.

Azo compounds

Ogawara et al.[84] reported an X-ray activable fluorescent probe (AZO-rhodamine 2, Fig. 3i), in which diethyl rhodamine and an electron-rich moiety were linked by an azo bond. The two-electron reduction of AZO-rhodamine 2 by aqueous electrons resulted in the release of diethyl rhodamine, via a hydrazine intermediate. The radiolytic yield of released rhodamine was ~0.14 μM Gy^{-1} in deoxygenated water containing 40% methanol. In-cell activation of AZO-rhodamine 2 showed a linear increase of fluorescence intensity as a function of radiation dose, indicating an efficient reaction of the azo bond with aqueous electrons.

Metal ions

The one-electron reduction of metal ions by aqueous electrons presents significant opportunities for researchers to investigate hyporeduced metal ions. Ahn et al.[85] reported the first example of cobalt(III) metal complexes whose stability markedly decreased under one-electron reduction by e^-_{aq}, resulting in the release of coordinated ligands. In a Co(cyclen)(8-HQ) complex (Fig. 4a), cyclen (1,4,7,10-tetraazacyclotetradecane) helps to tune the reductive potential of Co(III) and the drug model 8-HQ is released upon reduction of the metal centre. Under γ-rays activation in deoxygenated human plasma, G(8-HQ) was 0.17 μmol J^{-1}. Akisawa et al.[86] reported that, under hypoxic irradiation of an aqueous solution containing Cu(II), azide and acetylene, an azide–alkyne coupling reaction occurred (Fig. 4b). This reaction was catalysed by Cu(I), which was formed through the reduction of Cu(II) by e^-_{aq}. They also demonstrated that, owing to the deep penetration of X-rays, the reaction could still be initiated, even though the reacting vessels were inserted in pork meat. Wang et al.[87] reported a palladium pre-catalyst composed of Pd(II)$(OAc)_2$ and a porous organic polymer (Fig. 4c). Under irradiation in water, the reduction of Pd(II) to Pd(0) occurred, which then catalysed the Tsuji–Trost hydrolysis of

allyloxycarbonyl-caged Dox. Notably, they measured the *G*-value of the released drug to be 2.75 μM Gy^{-1}, approximately 10 times higher than that of e^-_{aq}. This finding suggests that the strategy of activating metal catalysts under irradiation can overcome the low-yield limitation of primary species, thereby enhancing radiation-induced reactions. Fu et al.[88] demonstrated that a Pt(IV) complex could be reduced by e^-_{aq}, leading to the dissociation of axial ligands and a Pt(II) complex (Fig. 4d). Using physiological stable prodrug OxaliPt(IV)-$(OAc)_2$ and the treatment with prodrug and 4 Gy X-rays showed enhanced cell-killing efficiency to a series of cell lines including HCT116, LoVo, Ls513 and HT29. Furthermore, as the ligands are cleaved when Pt(IV) is reduced to Pt(II), they designed an ADC, OxaliPt(IV)-ADC, using Pt(IV) as the linker of monoclonal anti-HER2 antibody trastuzumab and a cleavable MMAE as the axial ligand. Upon irradiation, the reduction of Pt(IV) led to the release of two types of antitumour drug, OxaliPt(IV) and MMAE. Mice bearing BGC823 or MC38 cells treated with ADC and X-rays showed better treatment efficiency while having no side effects (neither body weight loss nor abnormalities in major organs) when compared with control groups.

Dihydroxylbenzyl compounds

Fu et al.[89] reported a dihydroxylbenzyl-caged prodrug (Fig. 5a) in which the hydroxylation by hydroxyl radical could result in the cleavage of the protecting group. The di-substituted hydroxyl group makes the benzene ring more electron-rich, thus facilitating the electrophilic substitution by hydroxyl radical. A prodrug (Fig. 5) comprising this group and the antitumour drug MMAE showed drug release with a *G*-value of 0.04 μM Gy^{-1}. Cancer cells (4T1 cell line) treated with 10 nM prodrug and 4 Gy X-ray demonstrated significantly lower viability compared with prodrug or radiation treatment only.

Benzothiazoline compounds

Tuo et al.[90] demonstrated that *N*-substituted benzothiazolines (Fig. 5b) were sensitive to reactive oxygen species such as hydroxyl radical and super oxide. Hydroxyl radical or super oxide generated from water radiolysis can abstract a hydrogen radical from benzothiazoline to form an unstable benzylic radical, which loses an electron to form a benzothiazolium ion. The intermediate then is hydrolysed to release benzothiazole and carboxylic acid. The benzothiazolines react rapidly with oxygen-centred radicals (hydroxyl radical, alkylperoxyl radical and superoxide ion) while they are relatively inert to other oxidants (hypochlorite, $^1O_2$ and H_2O_2). Although the radiolytic yield of oxidation and the activation efficiency in biological environments were not determined, this study presents an alternative approach for designing radiation-induced oxidation-sensitive prodrugs.

Chalcogen compounds

Organic chalcogen compounds are reported to show response to reductants or oxidants in living systems and have been used in redox-responsive drug carriers[91–96]. Ma et al.[97] first applied the diselenide group in the design of an ionizing radiation-sensitive drug carrier (Fig. 6a). They hypothesized that the cleavage of the diselenide bond was initiated by hydroxyl radicals, which was confirmed using electron spin resonance. They incorporated the diselenide group in a polyethylene glycol poly urethane block co-polymer (PEG-PUSeSe-PEG), which formed nano-aggregates in aqueous solution. Upon 5 Gy of X-ray

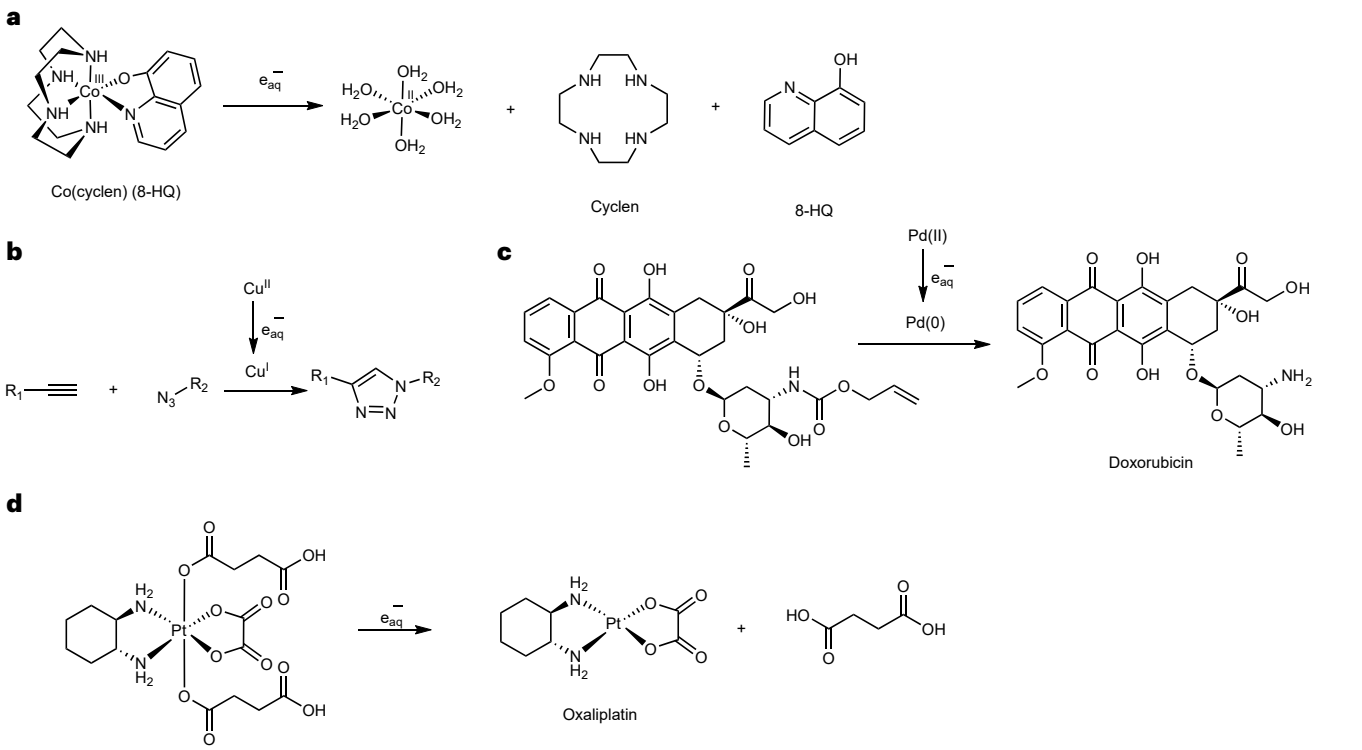

Fig. 4 | Radiation-induced reduction of metal ions to lower valence state under hypoxic conditions. a, Reduction of Co(III) complex by e^-_{aq} and the release of 8-HQ. **b**, Azide–alkyne click reaction catalysed by radiation-generated Cu(I). **c**, Pd(0) catalysed hydrolysis of allyloxycarbonyl-caged Dox in which the Pd(0) is generated by reaction of Pd(II) and e^-_{aq}. **d**, Reduction of Pt(IV) complex by e^-_{aq} and cleavage of the complex.

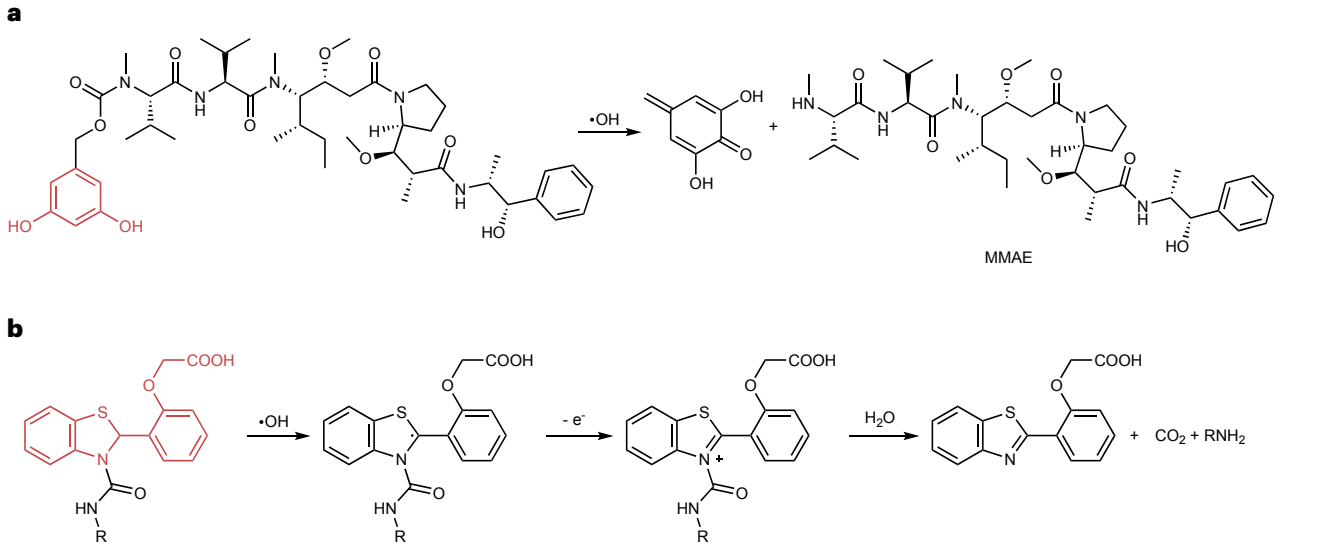

Fig. 5 | Prodrug activation induced by ·OH. a, Hydroxylation of dihydroxylbenzyl group-induced cleavage of self-immolative carbamate group. **b**, ·OH-activated benzothiazoline-based caging group and the release of amines. MMAE, monomethyl auristatin E.

irradiation, the nanocarrier could release up to 40% of the encapsulated doxorubicin. Using diselenide as the reactive group, the same group later reported radiation-sensitive hydrogels and liposomes[98]. However, the dose required to break the hydrogels were too high for clinical application. As a homologue of selenium, tellurium is also sensitive to redox stimuli[99]. Cao et al.[100] reported an amphiphilic polymer containing organic tellurium bond in the hydrophobic block (Fig. 6b). In response to only 2 Gy γ-irradiation, the micelles formed from the polymer swelled from 30 nm to around 200 nm as the oxidation of tellurium made the hydrophobic core more hydrophilic. This unique property made the polymer promising for applications in radiation-triggered drug release.

Disulfide bonds are reported to undergo one-electron reduction reactions leading to disulfide bond cleavage and exchange reactions. Tanabe et al.[101,102] demonstrated that disulfide bonds incorporated within an oligoDNA ampliphile could react with e^-_{aq} (Fig. 6c). The generated disulfide radical anion ($RSSR'^{\cdot -}$) decomposes into a sulfide anion (RS^-) and thiyl radical (RS·). The sulfide anion underwent disulfide exchange reaction with another molecule of disulfide. With this reaction, they designed a DNA amphiphile with a disulfide bond as the linker of the hydrophobic and hydrophilic block[103]. The polymer formed micelles in water with drugs encapsulated in the hydrophobic region. Under hypoxic X-irradiation, the disulfide exchange resulted in the disassembly of the micelle and release of the payload. A549 cell line treated with camptothecin-loaded micelles and 9 Gy X-irradiation under hypoxic conditions showed higher toxicity than without radiation.

Organochlorides

Organochlorides such as carbon tetrachloride and chloroform are reported to undergo one-electron reduction with e^-_{aq} to form a chlorocarbon radical and a chloride anion. Similar methods are used to treat organochloride-contaminated wastewater. Our group found that in aerobic solutions, the formed chlorocarbon radical will react with molecular oxygen to form a peroxyl radical, which can oxidize the double bond of a stilbene molecule[104] (Fig. 6d). Mechanistic studies unveiled that the yield of peroxyl radical depends on the molar ratio of dissolved oxygen and organochloride, where 2% oxygen resulted in an optimal yield of peroxyl radical[105]. We demonstrated that the organochloride peroxyradical can cleave an amphiphilic block co-polymer that has a stilbene group as the linker between the hydrophobic and hydrophilic blocks. Dox-loaded stilbene-block co-polymer micelles released 74% of encapsulated Dox after 15 Gy of X-irradiation in PBS containing 1 vol% chloroform. Furthermore, we found that hydrophilic organochloride-functionalized polymers functioned similar to small molecular organochlorides and that thioether compounds can also be oxidized to sulfoxides by the organochloride-mediated reaction[106]. Irradiation of a solution of hydrophilic co-polymer rP2 (Fig. 6e) led to oxidation of the thioether moieties to sulfoxide, initiating hydrolysis of the attached ester bond. This study indicates that the source of organochloride is not limited to highly toxic small-molecule organochlorides, paving the way to clinical application of this approach.

Radionuclide-activated prodrugs

So far, we have discussed the prodrug activation triggered by external radiation such as X-rays and γ-rays. It should be noted that radionuclides used in radiopharmaceuticals can also induce water radiolysis, creating radical products that can activate prodrugs. However, radionuclide application was not reported until Liu's group[107] demonstrated a 2-[^{18}F]-fluoro-2-deoxy-D-glucose ([^{18}F]FDG)-activated OxaliPt(IV) complex, in which a coumarin derivative was used as one of the axial ligands (Fig. 7a). After incubating [^{18}F]FDG with the Pt(IV) complex, they observed regeneration of coumarin fluorescence, suggesting the reduction of Pt(IV) complex and the release of the axial ligand. They designed a fibroblast activation protein-targeted ADC, sibrotuzumab-OxaliPt(IV)-MMAE (Pt-ADC, Fig. 7b), in which Pt(IV) was used as the linker of the antibody and MMAE. Co-treatment of 0.05 mCi [^{18}F]FDG and Pt-ADC demonstrated similar viability against 4T1-FAP cells compared with MMAE-treated group. For in vivo experiments on 4T1-FAP-bearing BALB/c mice, Pt-ADC was injected 2 days

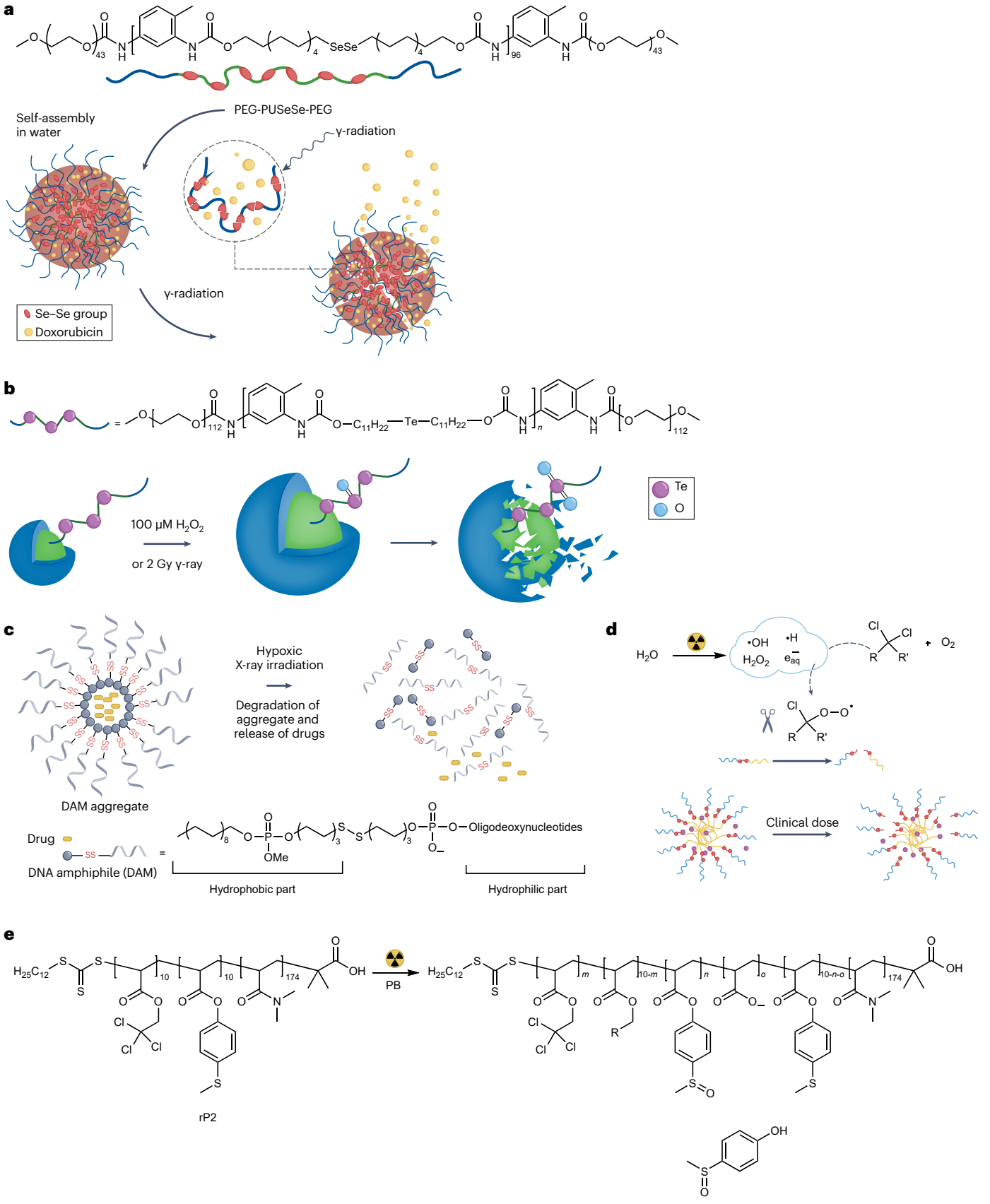
a
PEG-PUSeSe-PEG
Self-assembly in water
γ-radiation
γ-radiation
Se–Se group
Doxorubicin
b
100 μM H2O2
or 2 Gy γ-ray
Te
O
c
Hypoxic X-ray irradiation
Degradation of aggregate and release of drugs
DAM aggregate
Drug
DNA amphiphile (DAM)
OMe
Oligodeoxynucleotides
Hydrophobic part
Hydrophilic part
d
H2O
•OH
•H
H2O2
eaq
+ O2
Clinical dose
e
PB
rP2

Fig. 6 | Radiation-induced micelle disassembly. a, γ-radiation-induced oxidative cleavage of diselenide bond. **b**, Radiation-induced oxidation of tellurium-containing polymer. **c**, Hypoxic X-ray irradiation-induced disulfide exchange reaction. **d**, Organochloride-mediated oxidation induced by radiation. **e**, Polymer organochloride-mediated oxidation of thioethers. PB, phosphate buffer. Part **a** reprinted (adapted) with permission from ref. 97, ACS; part **b** adapted with permission from ref. 100, RSC; part **c** reprinted (adapted) with permission from ref. 103, ACS; part **d** adapted with permission from ref. 104, CCS; part **e** adapted from ref. 106, CC BY 4.0.

before administering 1 mCi [^{18}F]FDG to increase the antibody concentration at the tumour site. The Pt-ADC + [18F]FDG group showed four times higher MMAE concentration at the tumour site compared with that of the Pt-ADC single-treatment group. As a result, the co-treatment group showed a significant inhibition of tumour regrowth. In the following work of Liu's group[108], different radionuclides (such as ^{18}F, ^{68}Ga, ^{86}Y, ^{89}Zr and ^{177}Lu) were used to trigger drug release from the same complex (Fig. 7c). The drug activation appeared to have a linear response with absorbed dose (simulated dose calculated using Geant4 software), which was determined by the type of radiation, energy of radiation and the half-life of the radionuclide. Notably, ^{177}Lu induced the most prodrug activation in 48 h among all tested radionuclides. PKU525, an antibody designed for FAP-targeted radionuclide therapy, was labelled with ^{177}Lu and used in combination with Pt(IV)-Gem (Fig. 7d) to treat 4T1-FAP-bearing mouse. Co-treatment of [^{177}Lu]Lu-PKU525 and Pt(IV)-Gem showed remarkable tumour growth inhibition of solid tumours and extended survival rate for mice with metastatic tumour model. Quintana et al.[109] further studied more radionuclides on the efficiency of prodrug activation, using the *para*-azido-2,3,5,6-tetrafluorobenzyl moiety as the caging group. The activation efficiency varied 70-fold among different radionuclides (^{99m}Tc > ^{111}In > ^{177}Lu > ^{64}Cu > ^{32}P > ^{68}Ga > ^{223}Ra > ^{18}F), in which ^{99m}Tc showed 0.32 μM prodrug activation per Gy of exposure. The authors hypothesized that the low-energy electrons from radionuclide decay enabled more efficient drug activation than external beam radiation, as low-energy electrons could induce a higher concentration of ionizing events and increase the probability of local activation of macromolecules. In vivo experiments were performed on TBP3743 (FAP-expressing tumour)-bearing mice, in which

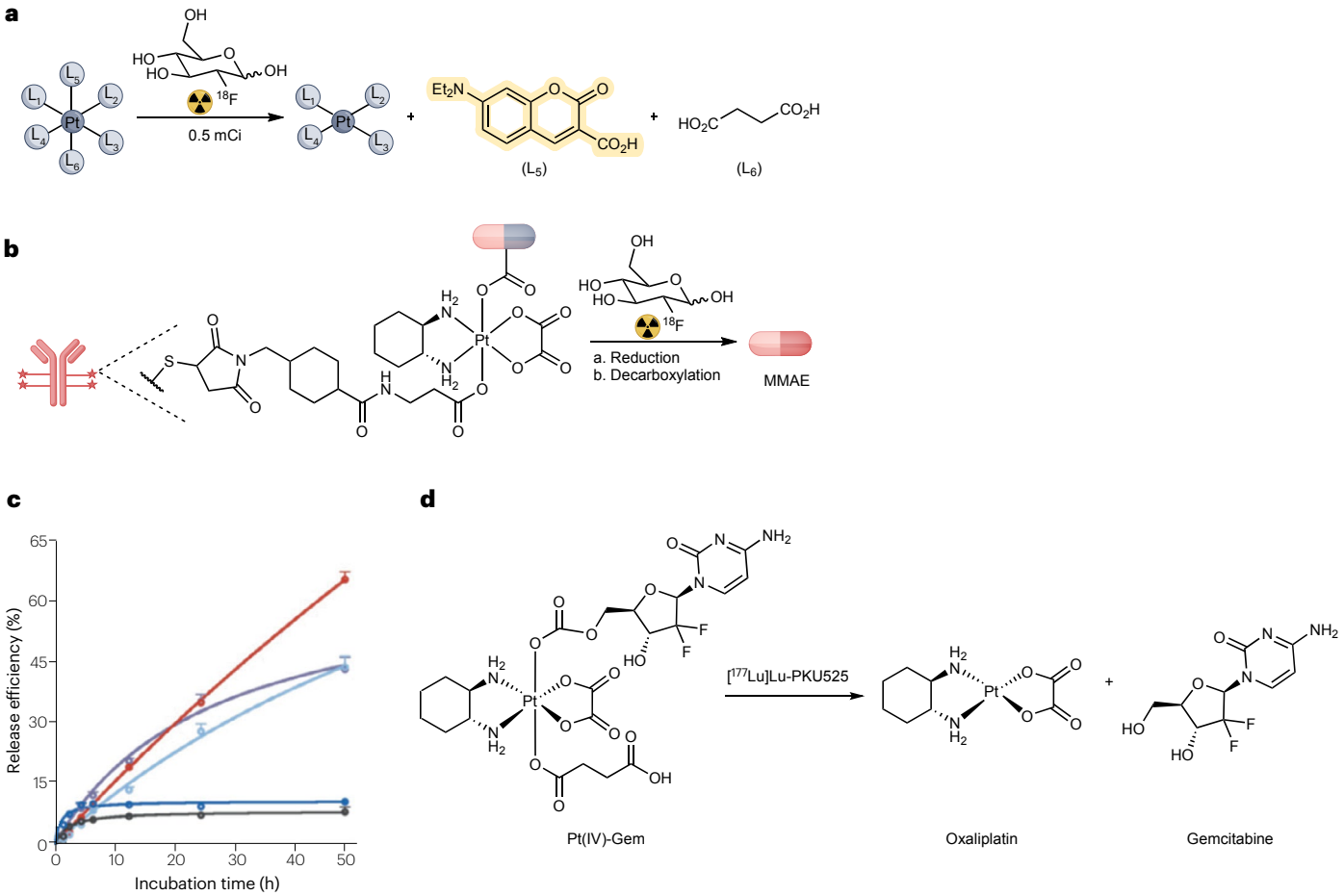

Fig. 7 | Radionuclides can deliver radiation leading to prodrug activation. **a**, Radiation from 2-[^{18}F]-fluoro-2-deoxy-D-glucose ([^{18}F]FDG)-induced Pt(IV) reduction and release of axial ligands. **b**, Structure of Pt-antibody–drug conjugate and [^{18}F]FDG-induced release of monomethyl auristatin E (MMAE). **c**, Release efficiency from a Pt(IV)-complex in response to different radionuclides. **d**, [^{177}Lu]Lu-PKU525-induced reduction of Pt(IV) complex and release of oxaliplatin and gemcitabine. Part **b** adapted with permission from ref. 107, Elsevier; part **c** adapted from ref. 108, CC BY 4.0.

co-treatment of [^{99m}Tc]Tc-FAP and Cy5-fluorescent albumin-conjugated caged MMAE showed high fluorescence signal and accumulation of MMAE in the tumour.

Although so far there are just a few papers on the use of radionuclides, this approach opens many exciting new opportunities. One option is to activate drugs using imaging radionuclides such as ^{18}F and ^{99m}Tc, which are commonly applied in diagnostics and which per definition impose low radiation burden to patients. In cases in which larger doses are needed, the use of typical therapeutic radionuclides such as ^{177}Lu or ^{131}I can enable combined radionuclide therapy with chemotherapy or immunotherapy.

Conclusions

Ionizing radiation-induced drug release offers a unique way to reduce the side effects of chemotherapeutic drugs. In this concept, radiation is used for both treatment and as an external stimulus to trigger drug release. The deep penetrating characteristic of radiation makes this strategy applicable to tumours deeply situated in the body. Radiation-induced drug release is mediated by reactive species generated from water radiolysis. The challenges associated with this concept are the low radiolytic yield of the reactive species (a few micromolar per radiation dose) and the side reactions of these species with a wide range of biological substances. Significant progress has been made in recent years to develop efficient releasing systems that can respond to clinical doses of radiation. Most of the reactive species generated in water radiolysis have been studied to trigger drug release. Hydroxyl radicals, as the most abundant species from water radiolysis, suffer from high reactivity with many cellular components, making it only applicable to highly sensitive functional groups such as diselenide, organotellurium and dihydroxylbenzyl compounds. Aqueous electrons have drawn more attention than other species because of the relatively higher yield and selective reactivity towards a few functional groups such as *N*-oxide, organoazides, carbon–halogen bond and picolinium groups. Moreover, the reduction of metal ions by aqueous electrons brings new approaches of activating drugs in cancerous tissues, and associated metal-catalysed reactions may potentially enable drug release exceeding the maximum yield of radiolysis products.

Published online: 15 December 2025

References

1. Denkova, A. G., Liu, H., Men, Y. & Eelkema, R. Enhanced cancer therapy by combining radiation and chemical effects mediated by nanocarriers. *Adv. Ther.* **3**, 1900177 (2020).
2. Anand, U. et al. Cancer chemotherapy and beyond: current status, drug candidates, associated risks and progress in targeted therapeutics. *Genes Dis.* **10**, 1367–1401 (2023).
3. Makin, G. Principles of chemotherapy. *Paediatr. Child Health* **28**, 183–188 (2018).
4. Begg, A. C., Stewart, F. A. & Vens, C. Strategies to improve radiotherapy with targeted drugs. *Nat. Rev. Cancer* **11**, 239–253 (2011).
5. Xu, X. D. et al. Ultra-pH-responsive and tumor-penetrating nanoplatform for targeted siRNA delivery with robust anti-cancer efficacy. *Angew. Chem. Int. Ed.* **55**, 7091–7094 (2016).
6. Guo, J. S. et al. Dual hypoxia-responsive supramolecular complex for cancer target therapy. *Nat. Commun.* **14**, 5634 (2023).
7. Wang, B. et al. Potent and prolonged innate immune activation by enzyme-responsive imidazoquinoline TLR7/8 agonist prodrug vesicles. *J. Am. Chem. Soc.* **142**, 12133–12139 (2020).
8. Zhang, W. et al. Light-triggered release of conventional local anesthetics from a macromolecular prodrug for on-demand local anesthesia. *Nat. Commun.* **11**, 2323 (2020).
9. Tu, L. et al. Ultrasound-controlled drug release and drug activation for cancer therapy. *Exploration* **1**, 20210023 (2021).
10. Ding, C. D., Chen, C. B., Zeng, X. W., Chen, H. Z. & Zhao, Y. L. Emerging strategies in stimuli-responsive prodrug nanosystems for cancer therapy. *ACS Nano* **16**, 13513–13553 (2022).
11. Read, G. H., Bailleul, J., Vlashi, E. & Kesarwala, A. H. Metabolic response to radiation therapy in cancer. *Mol. Carcinog.* **61**, 200–224 (2022).
12. Zhang, L. et al. Chemotherapy plus radiotherapy versus radiotherapy alone in patients with anaplastic glioma: a systematic review and meta-analysis. *J. Cancer Res. Clin. Oncol.* **139**, 719–726 (2013).
13. Lonati, L., Barbieri, S., Guardamagna, I., Ottolenghi, A. & Baiocco, G. Radiation-induced cell cycle perturbations: a computational tool validated with flow-cytometry data. *Sci. Rep.* **11**, 925 (2021).
14. Xu, Z. et al. Nanoscale metal-organic framework with an X-ray triggerable prodrug for synergistic radiotherapy and chemotherapy. *J. Am. Chem. Soc.* **145**, 18698–18704 (2023).
15. Zhen, W. et al. Nanoscale mixed-ligand metal-organic framework for X-ray stimulated cancer therapy. *J. Am. Chem. Soc.* **146**, 33149–33158 (2024).
16. Shi, Y. et al. Localized nuclear reaction breaks boron drug capsules loaded with immune adjuvants for cancer immunotherapy. *Nat. Commun.* **14**, 1884 (2023).
17. Cao, W., Gu, Y., Meineck, M. & Xu, H. The combination of chemotherapy and radiotherapy towards more efficient drug delivery. *Chem. Asian J.* **9**, 48–57 (2014).
18. Liu, H. et al. Ionizing radiation-induced release from poly(ε-caprolactone-b-ethylene glycol) micelles. *ACS Appl. Polym. Mater.* **3**, 968–975 (2020).
19. Liu, H. et al. Combined chemoradionuclide therapy using poly(ε-caprolactone-b-ethylene oxide) micelles as the delivery vehicle. *Adv. Ther.* **6**, 2200224 (2023).
20. Li, X., Sun, H., Lu, Y. & Xing, L. Radiotherapy-triggered prodrug activation: a new era in precise chemotherapy. *Med* **3**, 600–602 (2022).
21. Farrer, N. J., Higgins, G. S. & Kunkler, I. H. Radiation-induced prodrug activation: extending combined modality therapy for some solid tumours. *Br. J. Cancer* **126**, 1241–1243 (2022).
22. Kamkaew, A., Chen, F., Zhan, Y., Majewski, R. L. & Cai, W. Scintillating nanoparticles as energy mediators for enhanced photodynamic therapy. *ACS Nano* **10**, 3918–3935 (2016).
23. Sun, W. et al. Nanosensitizer-mediated unique dynamic therapy tactics for effective inhibition of deep tumors. *Adv. Drug Deliv. Rev.* **192**, 114643 (2023).
24. Zhang, X. et al. Low-dose X-ray excited photodynamic therapy based on $NaLuF_4$:Tb^{3+}-rose bengal nanocomposite. *Bioconjug. Chem.* **30**, 2191–2200 (2019).
25. Tu, Z. et al. Porphyrin-engineered (125)I-nanoseeds as a prototype for immunogenic brachytherapy. *J. Am. Chem. Soc.* **147**, 13229–13242 (2025).
26. Cao, Y. et al. X-ray-triggered activation of polyprodrugs for synergistic radiochemotherapy. *Biomacromolecules* **26**, 579–590 (2025).
27. Kang, M. et al. Sustained and localized drug depot release using radiation-activated scintillating nanoparticles. *Adv. Mater.* **36**, e2312326 (2024).
28. Ruan, F. et al. Leveraging radiation-triggered metal prodrug activation through nanosurface energy transfer for directed radio-chemo-immunotherapy. *Angew. Chem. Int. Ed.* **63**, e202317943 (2024).
29. Guesdon-Vennerie, A. et al. Breaking photoswitch activation depth limit using ionising radiation stimuli adapted to clinical application. *Nat. Commun.* **13**, 4102 (2022).
30. Cao, Y., Si, J., Zheng, M., Zhou, Q. & Ge, Z. X-ray-responsive prodrugs and polymeric nanocarriers for multimodal cancer therapy. *Chem. Commun.* **59**, 8323–8331 (2023).
31. Liu, H. et al. X-ray-induced drug release for cancer therapy. *Angew. Chem. Int. Ed.* **62**, e202306100 (2023).
32. Fu, Q. et al. Bioorthogonal chemistry for prodrug activation in vivo. *Chem. Soc. Rev.* **52**, 7737–7772 (2023).
33. Jiang, R., Fang, Q., Liu, W., Chen, L. & Yang, H. Recent progress in radiosensitive nanomaterials for radiotherapy-triggered drug release. *ACS Appl. Mater. Interfaces* **17**, 14801–14821 (2025).
34. Wang, C., Zhang, Z. & Liu, Z. Radiotherapy-activated prodrug: past, present and beyond. *ACS Cent. Sci.* **11**, 1306–1320 (2025).
35. Richter, H. W. in *Photochemistry and Radiation Chemistry* 5–33 (American Chemical Society, 1998).
36. Buxton, G. V. in *Radiation Chemistry Principles and Applications* (eds Farhataziz & Rodgers, M. A. J.) 321–350 (VCH Publishers Inc., 1987).
37. Buxton, G. V. in *Radiation Chemistry* (eds Spotheim-Maurizot, M. et al.) 3–16 (EDP Sciences, 2008).
38. O'Neill, P. & Wardman, P. Radiation chemistry comes before radiation biology. *Int. J. Radiat. Biol.* **85**, 9–25 (2009).
39. Wardman, P. The importance of radiation chemistry to radiation and free radical biology (The 2008 Silvanus Thompson Memorial Lecture). *Br. J. Radiol.* **82**, 89–104 (2009).
40. Baldacchino, G. et al. Importance of radiolytic reactions during high-LET irradiation modalities: LET Effect, role of O_2 and radiosensitization by nanoparticles. *Cancer Nanotechnol.* **10**, 3 (2019).
41. LaVerne, J. A. Hydrated electron yields in the heavy ion radiolysis of water. *J. Phys. Chem. A* **109**, 9393–9401 (2005).
42. LaVerne, J. A. in *Charged Particle and Photon Interactions with Matter* (eds Mozumder, A. & Hatano, Y.) 27 (Dekker, 2004).
43. Wardman, P. Initiating redox reactions by ionizing radiation: a versatile, selective and quantitative tool. *Redox Biochem. Chem.* **5–6**, 100004 (2023).
44. Wu, H. Y. et al. Preoperative short-course radiotherapy followed by consolidation chemotherapy for treatment with locally advanced rectal cancer: a meta-analysis. *Radiat. Oncol.* **17**, 14 (2022).
45. Bernier, J. Alteration of radiotherapy fractionation and concurrent chemotherapy: a new frontier in head and neck oncology? *Nat. Clin. Pract. Oncol.* **2**, 305–314 (2005).
46. De Ruysscher, D. et al. Radiotherapy toxicity. *Nat. Rev. Dis. Prim.* **5**, 13 (2019).

47. Buxton, G. V., Greenstock, C. L., Helman, W. P. & Ross, A. B. Critical review of rate constants for reactions of hydrated electrons, hydrogen atoms and hydroxyl radicals (·OH/·O$^-$) in aqueous solution. *J. Phys. Chem. Ref. Data* **17**, 513–886 (1988).
48. Daily, R. & Minakata, D. Reactivities of hydrated electrons with organic compounds in aqueous-phase advanced reduction processes. *Environ. Sci. Water Res. Technol.* **8**, 543–574 (2022).
49. Daily, R. & Minakata, D. Development of a group contribution method to predict the aqueous-phase reactivities of hydrated electrons with organic compounds. *J. Adv. Chem. Eng.* **15**, 100493 (2023).
50. Minakata, D. Development of an elementary reaction-based kinetic model to predict the aqueous-phase fate of organic compounds induced by reactive free radicals. *Acc. Chem. Res.* **57**, 1658–1669 (2024).
51. Cadet, J., Angelov, D. & Wagner, J. R. Hydroxyl radical is predominantly involved in oxidatively generated base damage to cellular DNA exposed to ionizing radiation. *Int. J. Radiat. Biol.* **98**, 1684–1690 (2022).
52. Coussens, L. M. & Werb, Z. Inflammation and cancer. *Nature* **420**, 860–867 (2002).
53. Winterbourn, C. C. Reconciling the chemistry and biology of reactive oxygen species. *Nat. Chem. Biol.* **4**, 278–286 (2008).
54. Dong, C. et al. Self-assembly of oxidation-responsive polyethylene glycol-paclitaxel prodrug for cancer chemotherapy. *J. Control. Rel.* **321**, 529–539 (2020).
55. Skarbek, C., Serra, S., Maslah, H., Rascol, E. & Labruère, R. Arylboronate prodrugs of doxorubicin as promising chemotherapy for pancreatic cancer. *Bioorg. Chem.* **91**, 103158 (2019).
56. Anderson, A. R. & Hart, E. J. Molecular product and free radical yields in the decomposition of water by protons, deuterons, and helium ions. *Radiat. Res.* **14**, 689–704 (1961).
57. Pastina, B. & LaVerne, J. A. Hydrogen peroxide production in the radiolysis of water with heavy ions. *J. Phys. Chem. A* **103**, 1592–1597 (1999).
58. Wardman, P. Approaches to modeling chemical reaction pathways in radiobiology. *Int. J. Radiat. Biol.* **98**, 1399–1413 (2022).
59. Michaels, H. B. & Hunt, J. W. A model for radiation damage in cells by direct effect and by indirect effect: a radiation chemistry approach. *Radiat. Res.* **74**, 23–34 (1978).
60. Hwang, C., Sinskey, A. J. & Lodish, H. F. Oxidized redox state of glutathione in the endoplasmic reticulum. *Science* **257**, 1496–1502 (1992).
61. Lee, M. H. et al. Disulfide-cleavage-triggered chemosensors and their biological applications. *Chem. Rev.* **113**, 5071–5109 (2013).
62. Hassan, S. S. M. & Rechnitz, G. A. Determination of glutathione and glutathione reductase with a silver sulfide membrane electrode. *Anal. Chem.* **54**, 1972–1976 (1982).
63. Fu, X. et al. Cysteine disulfides (Cys-ss-X) as sensitive plasma biomarkers of oxidative stress. *Sci. Rep.* **9**, 115 (2019).
64. Kleinman, W. A. & Richie, J. P. Status of glutathione and other thiols and disulfides in human plasma. *Biochem. Pharmacol.* **60**, 19–29 (2000).
65. McKeown, S. R. Defining normoxia, physoxia and hypoxia in tumours-implications for treatment response. *Br. J. Radiol.* **87**, 20130676 (2014).
66. Koobotse, M. O., Schmidt, D., Holly, J. M. P. & Perks, C. M. Glucose concentration in cell culture medium influences the BRCA1-mediated regulation of the lipogenic action of IGF-I in breast cancer cells. *Int. J. Mol. Sci.* **21**, 8674 (2020).
67. Snider, J. W. et al. Cyberknife with tumor tracking: an effective treatment for high-risk surgical patients with single peripheral lung metastases. *Front. Oncol.* **2**, 63 (2012).
68. Okamoto, S. et al. Radiation dosimetry for ^{177}Lu-PSMA I&T in metastatic castration-resistant prostate cancer: absorbed dose in normal organs and tumor lesions. *J. Nucl. Med.* **58**, 445–450 (2017).
69. Shibamoto, Y., Zhou, L., Hatta, H., Mori, M. & Nishimoto, S. In vivo evaluation of a novel antitumor prodrug, 1-(2′-oxopropyl)-5-fluorouracil (OFU001), which releases 5-fluorouracil upon hypoxic irradiation. *Int. J. Radiat. Oncol. Biol. Phys.* **49**, 407–413 (2001).
70. Tanabe, K., Sugiura, M., Ito, T. & Nishimoto, S. Synthesis and one-electron reduction characteristics of radiation-activated prodrugs possessing two 5-fluorodeoxyuridine units. *Bioorg. Med. Chem.* **20**, 5164–5168 (2012).
71. Peng, H. J. et al. A fluorescent probe for fast and quantitative detection of hydrogen sulfide in blood. *Angew. Chem. Int. Ed.* **50**, 9672–9675 (2011).
72. Tanabe, K., Ishizaki, J., Ando, Y., Ito, T. & Nishimoto, S. Reductive activation of 5-fluorodeoxyuridine prodrug possessing azide methyl group by hypoxic X-irradiation. *Bioorg. Med. Chem. Lett.* **22**, 1682–1685 (2012).
73. Geng, J. et al. Switching on prodrugs using radiotherapy. *Nat. Chem.* **13**, 805–810 (2021).
74. Yang, C., Yang, Y., Li, Y., Ni, Q. & Li, J. Radiotherapy-triggered proteolysis targeting chimera prodrug activation in tumors. *J. Am. Chem. Soc.* **145**, 385–391 (2023).
75. Sun, J. et al. Radiation-activated resiquimod prodrug nanomaterials for enhancing immune checkpoint inhibitor therapy. *Nano Lett.* **24**, 2921–2930 (2024).
76. Wilson, W. R. & Hay, M. P. Targeting hypoxia in cancer therapy. *Nat. Rev. Cancer* **11**, 393–410 (2011).
77. Ding, Z. et al. Radiotherapy reduces *N*-oxides for prodrug activation in tumors. *J. Am. Chem. Soc.* **144**, 9458–9464 (2022).
78. Ding, Z. et al. Single atom engineering for radiotherapy-activated immune agonist prodrugs. *Nat. Commun.* **16**, 6021 (2025).
79. Yin, X. et al. Orchestrating intratumoral DC-T cell immunity for enhanced tumor control via radiotherapy-activated TLR7/8 prodrugs in mice. *Nat. Commun.* **16**, 6020 (2025).
80. Anderson, R. F., Sutherland, H. S. & Marshall, A. J. Chain-release of quinoline-based drugs from *N*-alkoxyquinoline prodrugs upon radiolytic one-electron reduction. *Chem. Commun.* **61**, 9968–9971 (2025).
81. Kriste, A. G., Tercel, M., Anderson, R. F., Ferry, D. M. & Wilson, W. R. Pathways of reductive fragmentation of heterocyclic nitroarylmethyl quaternary ammonium prodrugs of mechlorethamine. *Radiat. Res.* **158**, 753–762 (2002).
82. Guo, Z. et al. Radiotherapy-induced cleavage of quaternary ammonium groups activates prodrugs in tumors. *Angew. Chem. Int. Ed.* **61**, e202205014 (2022).
83. Fu, Q. et al. Radiotherapy activates picolinium prodrugs in tumours. *Nat. Chem.* **16**, 1348–1356 (2024).
84. Ogawara, K. et al. Theoretical design and synthesis of caged compounds using X-ray-triggered azo bond cleavage. *Adv. Sci.* **11**, e2306586 (2024).
85. Ahn, G. O., Ware, D. C., Denny, W. A. & Wilson, W. R. Optimization of the auxiliary ligand shell of cobalt(III)(8-hydroxyquinoline) complexes as model hypoxia-selective radiation-activated prodrugs. *Radiat. Res.* **162**, 315–325 (2004).
86. Akisawa, K., Makanai, H., Nishihara, T. & Tanabe, K. Hypoxic X-irradiation as a trigger for reduction of metal ion and azide-alkyne cycloaddition on oligodeoxynucleotides. *Tetrahedron Lett.* **92**, 153658 (2022).
87. Wang, J. et al. Radiotherapy mediated catalytic prodrug therapy with higher radiochemical conversion than hydrated electrons. Preprint at *ChemRxiv* https://doi.org/10.26434/chemrxiv-2024-p5r35-v2 (2024).
88. Fu, Q. et al. Radiotherapy-triggered reduction of platinum-based chemotherapeutic prodrugs in tumours. *Nat. Biomed. Eng.* **8**, 1425–1435 (2024).
89. Fu, Q. et al. External-radiation-induced local hydroxylation enables remote release of functional molecules in tumors. *Angew. Chem. Int. Ed.* **59**, 21546–21552 (2020).
90. Tuo, W. et al. Radiation-responsive benzothiazolines as potential cleavable fluorogenic linkers for drug delivery. *Chem. Eur. J.* **29**, e202300358 (2023).
91. Ma, N., Li, Y., Xu, H., Wang, Z. & Zhang, X. Dual redox responsive assemblies formed from diselenide block copolymers. *J. Am. Chem. Soc.* **132**, 442–443 (2010).
92. Li, T. et al. Diselenide-pemetrexed assemblies for combined cancer immuno-, radio-, and chemotherapies. *Angew. Chem. Int. Ed.* **59**, 2700–2704 (2020).
93. Li, T., Pan, S., Zhuang, H., Gao, S. & Xu, H. Selenium-containing carrier-free assemblies with aggregation-induced emission property combine cancer radiotherapy with chemotherapy. *ACS Appl. Bio. Mater.* **3**, 1283–1292 (2020).
94. Gao, S. Q. et al. Selenium-containing nanoparticles combine the NK cells mediated immunotherapy with radiotherapy and chemotherapy. *Adv. Mater.* **32**, e1907568 (2020).
95. Wu, Y. et al. Radioresponsive delivery of toll-like receptor 7/8 agonist for tumor radioimmunotherapy enabled by core-cross-linked diselenide nanoparticles. *ACS Nano* **18**, 2800–2814 (2024).
96. You, Y. et al. Cleavage of homonuclear chalcogen–chalcogen bonds in a hybrid platform in response to X-ray radiation potentiates tumor radiochemotherapy. *Angew. Chem. Int. Ed.* **64**, e202412922 (2025).
97. Ma, N. et al. Radiation-sensitive diselenide block co-polymer micellar aggregates: toward the combination of radiotherapy and chemotherapy. *Langmuir* **27**, 5874–5878 (2011).
98. Cao, W., Zhang, X., Miao, X., Yang, Z. & Xu, H. Gamma-ray-responsive supramolecular hydrogel based on a diselenide-containing polymer and a peptide. *Angew. Chem. Int. Ed.* **52**, 6233–6237 (2013).
99. Dai, Y. H. et al. Tellurium-containing polymers: recent developments and trends. *Prog. Polym. Sci.* **141**, 101678 (2023).
100. Cao, W., Gu, Y., Li, T. & Xu, H. Ultra-sensitive ROS-responsive tellurium-containing polymers. *Chem. Commun.* **51**, 7069–7071 (2015).
101. Tanabe, K., Matsumoto, E., Ito, T. & Nishimoto, S. Radiolytic cyclization of stem-and-loop structured oligodeoxynucleotide with neighboring arrangement of alpha, omega-bis-disulfides. *Org. Biomol. Chem.* **8**, 4837–4842 (2010).
102. Tanabe, K., Kuraseko, E., Yamamoto, Y. & Nishimoto, S.-I. One-electron reductive template-directed ligation of oligodeoxynucleotides possessing a disulfide bond. *J. Am. Chem. Soc.* **130**, 6302–6303 (2008).
103. Tanabe, K., Asada, T., Ito, T. & Nishimoto, S. Radiolytic reduction characteristics of drug-encapsulating DNA aggregates possessing disulfide bond. *Bioconjug. Chem.* **23**, 1909–1914 (2012).
104. Liu, J. et al. Organochlorides mediate oxidation reactions induced by low dose ionizing radiation. *CCS Chem.* **6**, 1712–1720 (2024).
105. Liu, J. et al. Reaction network analysis of organochloride mediated oxidation induced by ionizing radiation. Preprint at *ChemRxiv* https://doi.org/10.26434/chemrxiv-2025-cq53z (2025).
106. Liu, J., Piergentili, I., Xu, B., Denkova, A. G. & Eelkema, R. Alkyl chloride-functionalized polymers mediate oxidation of thioethers initiated by ionizing radiation. *ACS Appl. Polym. Mater.* **7**, 3835–3841 (2025).
107. Wang, C. et al. Locally unlocks prodrugs by radiopharmaceutical in tumor for cancer therapy. *Sci. Bull.* **69**, 2745–2755 (2024).
108. Guo, Z. et al. Targeted radionuclide therapy activates prodrugs for treating metastasis. *ACS Cent. Sci.* **10**, 2321–2330 (2024).
109. Quintana, J. M. et al. Localized in vivo prodrug activation using radionuclides. *J. Nucl. Med.* **66**, 91–97 (2025).
110. Shibamoto, Y., Zhou, L., Hatta, H., Mori, M. & Nishimoto, S. A novel class of antitumor prodrug, 1-(2′-oxopropyl)-5-fluorouracil (OFU001), that releases 5-fluorouracil upon hypoxic irradiation. *Jpn. J. Cancer Res.* **91**, 433–438 (2000).
111. Hart, E. J., Gordon, S. & Thomas, J. K. Rate constants of hydrated electron reactions with organic compounds. *J. Phys. Chem.* **68**, 1271–1274 (1964).

Acknowledgements
J.L. thanks the Chinese Scholarship Council for funding.

Author contributions
J.L. was responsible for researching data for the article and wrote the article, with contributions from A.G.D. and R.E. All authors discussed the content and provided input on the final version.

Competing interests
The authors declare no competing interests.

Additional information
Supplementary information The online version contains supplementary material available at https://doi.org/10.1038/s41570-025-00779-3.

Peer review information *Nature Reviews Chemistry* thanks Zhibo Liu and the other, anonymous, reviewer(s) for their contribution to the peer review of this work.